Comprehensive evaluation of zwitterionic hydrophilic liquid chromatography stationary phases for oligonucleotide characterization

Lardeux, Honorine; Guillarme, Davy; D'Atri, Valentina

How to cite

LARDEUX, Honorine, GUILLARME, Davy, D’ATRI, Valentina. Comprehensive evaluation of zwitterionic hydrophilic liquid chromatography stationary phases for oligonucleotide characterization. In: Journal of chromatography, 2023, vol. 1690, p. 463785. doi: 10.1016/j.chroma.2023.463785

This publication URL: https://archive-ouverte.unige.ch/unige:168294
Publication DOI: 10.1016/j.chroma.2023.463785

Journal of Chromatography A 1690 (2023) 463785

Contents lists available at ScienceDirect

Journal of Chromatography A

journal homepage: www.elsevier.com/locate/chroma

Comprehensive evaluation of zwitterionic hydrophilic liquid chromatography stationary phases for oligonucleotide characterization

Honorine Lardeux[a,b], Davy Guillarme[a,b], Valentina D'Atri[a,b,*]

[a] Institute of Pharmaceutical Sciences of Western Switzerland (ISPSO), University of Geneva, CMU-Rue Michel Servet 1, 4, Geneva 1211, Switzerland
[b] School of Pharmaceutical Sciences, University of Geneva, CMU-Rue Michel Servet 1, 4, Geneva 1211, Switzerland

ARTICLE INFO

Article history:
Received 31 October 2022
Revised 5 January 2023
Accepted 7 January 2023
Available online 8 January 2023

Keywords:
Hydrophilic interaction chromatography
Selectivity
Oligonucleotides
Zwitterionic stationary phases

ABSTRACT

Hydrophilic interaction chromatography (HILIC) has been proposed as a valuable alternative to ion-pairing reversed-phase chromatography (IP-RPLC) for oligonucleotide (ON) analysis. In this context, the potential of seven zwitterionic HILIC columns has been evaluated against amide- and poly-hydroxy fructan-functionalized HILIC columns and a C18 column operated under IP-RPLC mode.

Based on the retention characteristics of key small molecule pairs, each zwitterionic HILIC column showed a unique radar-shaped profile, suggesting different selectivities for distinct structural differences. Unmodified DNA and RNA samples were then evaluated, and the columns classified based on their retentivity. Two zwitterionic columns were particularly promising in terms of overall resolution, especially for the largest ONs (> 40-mer). Finally, separations between a chemically modified drug-like ON and its closely related impurities were performed. Although the ZIC-cHILIC column showed similar selectivity values as compared to the reference IP-RPLC technique, all columns demonstrated a general decrease in selectivity due to the minor structural differences present in the highly complex samples.

This work highlights the utility of zwitterionic HILIC mode for ON analysis and it reveals the importance of understanding columns characteristics – in terms of retention and selectivity – when selecting a stationary phase for specific ON applications.

1. Introduction

Therapeutic oligonucleotides (ONs) can modulate the function of specific proteins associated with disease states or pathogenicity by manipulating gene expression at translational level [1,2]. For this reason, they are emerging as successful drugs for addressing unmet medical needs, such as the treatment of genetically well-defined rare diseases [3]. Although the concept at the base of their therapeutic potential was known from long time, improvements in ONs stability and pharmacokinetic properties (especially in the form of chemical modifications) has drastically increased the chances of ONs to go from bench to bedside [4,5]. By the second quarter of 2022, 17 therapeutic ONs have been approved by Food and Drug Administration (FDA) or European Medicines Agency (EMA), with 13 of them (all chemically modified) in the single period 2016 – 2022 [4,6,7].

In this context, chemical modifications applied to ONs (involving all the components of the nucleotide, specifically the sugar moiety, the phosphate linkage, and the nitrogen base) have resulted in a wider diversity of impurities and structural variability that need to be addressed, in terms of analytical characterization [8,9]. Liquid chromatography (LC) is firmly positioned as the preferred analytical approach for identity and purity assessment, and ion-pairing reversed-phase liquid chromatography (IP-RPLC) is the most widely used LC mode [10–12]. Besides, hydrophilic liquid chromatography (HILIC) has emerged as a viable alternative chromatographic approach [13–17]. Silica-, diol-, and amide-bonded HILIC columns have been successfully applied for the separation of unmodified and phosphorothioated ONs [14,16–18]. ONs presenting methylated nucleobases such as 5-methylcytosine (mC) or sugar moiety modifications such as 2′-*O*-methyl (OMe), 2′-*O*-methoxyethyl (MOE), and locked nucleic acid (LNA), have also been investigated under HILIC conditions by using different types of columns packing materials [13,15,16]. Although zwitterionic HILIC columns were sporadically included in these studies, the potential of this HILIC mode for the analysis of ONs has not yet been systematically evaluated.

---

[*] Corresponding author at: Institute of Pharmaceutical Sciences of Western Switzerland (ISPSO), School of Pharmaceutical Sciences, University of Geneva, CMU - Rue Michel Servet 1, 4, Geneva 1211, Switzerland.
E-mail address: valentina.datri@unige.ch (V. D'Atri).

https://doi.org/10.1016/j.chroma.2023.463785

Zwitterionic stationary phases generally include (but are not limited to) derivatization with sulfobetaine groups bearing sulfonate and quaternary ammonium groups in a 1:1 molar ratio resulting in a net-zero surface charge [19]. This particular bonding allows a weak ion-exchange behavior together with a high affinity for polar neutral substances in HILIC that could be exploited for the analysis of charged/polar compounds, such as ONs [13,19]. In this contribution, seven zwitterionic columns (six derivatized with sulfobetaine groups and one with phosphorylcholine) were systematically compared to amide- and poly-hydroxy fructan (OH5)-functionalized HILIC phases and to a C18 stationary phase used under IP-RPLC conditions. First, all HILIC columns were screened with the Tanaka test to characterize the critical parameters that dictate the key interactions: hydrophobicity, hydrophilicity, shape/steric selectivity, hydrogen bonding, ion exchange, and acidic-basic nature of the stationary phase. Then, the analyses were performed on both unmodified and extremely chemically modified samples mimicking the "complexity" of the commercialized therapeutic ON volanesorsen (Waylivra®). With the goal to mimic the possible active pharmaceutical ingredient (API) impurities of this sample, ONs differing in terms of phosphodiester impurities, sequence length, number of 5-methylcytosine or MOE sugar moiety modifications were evaluated.

To our knowledge, this is the first comprehensive study conducted for the analysis of different chemically modified ONs under zwitterionic HILIC mode.

2. Materials and methods

2.1. Chemicals and reagents

2.1.1. Chemical and reagents for Tanaka test

Type 1 water was obtained from a Milli-Q purification system from Millipore (Bedford, MA, USA). LC-MS grade acetonitrile and uridine (U, 99%) were purchased from Thermo Fisher Scientific (Reinach, Switzerland). 2′-deoxyguanosine monohydrate (2d, ≥99%), 2′-deoxyuridine (2dU, ≥98.5%), 5-methyluridine (5MU, 97%), acetic acid (AA, ≥99%), adenosine (A, ≥99%), ammonium acetate solution 5 M (BioUltra), N,N,N-trimethylphenylammonium chloride (TMPAC, ≥98%), sodium *p*-toluenesulfonate (SPTS, 95%), theobromine (Tb, ≥98%), theophylline (Tp, ≥99%), toluene for HPLC (99.9%) and vidarabine monohydrate (V) were purchased from Sigma-Aldrich (Buchs, Switzerland). 3′-deoxyguanosine (3d, ≥95%) was purchased from Brunschwig (Basel, Switzerland).

2.1.2. Chemical and reagents for oligonucleotide analyses

Oligonucleotides were purchased from Eurogentec (Seraing, Belgium) and Integrated DNA Technologies (IDT, Leuven, Belgium). Type 1 water was obtained from a Milli-Q purification system from Millipore. LC-MS grade methanol and acetonitrile were purchased from Thermo Fisher Scientific (Reinach, Switzerland). Ammonium acetate solution 5 M (BioUltra), 1,1,1,3,3,3-hexafluoro-2-propanol (HFIP, ≥99%), triethylamine (TEA, ≥99.5%), and RNase-free water were purchased from Sigma-Aldrich (Buchs, Switzerland).

2.2. Sample information

Eppendorf DNA LoBind® tubes, Eppendorf Dualfilter T.I.P.S® and polypropylene vials were systematically used during this work.

2.2.1. Samples for Tanaka test

Stock solutions of each compound were initially prepared at 1 mg/mL by dissolving 1 mg of analyte in 1 mL of mobile phase (see Section 2.4.1). Toluene solution (1 mg/mL) was used as t_0 marker and prepared by diluting 1.45 µL of toluene in 1 mL of mobile phase. The test mixtures comprised selected pairs of compounds that were expected to vary in their interactions with the stationary phases, plus the t_0 marker. A total of seven mixtures (0.33 mg/mL) were prepared: test mixture 1: t_0, uridine (U), 5-methyluridine (5MU); test mixture 2: t_0, uridine (U), 2′-deoxyuridine (2dU); test mixture 3: t_0, adenosine (A), vidarabine (V); test mixture 4: t_0, 2′ deoxyguanosine (2d), 3′- deoxyguanosine (3d); test mixture 5: t_0, uridine (U), sodium p-toluenesulfonate (SPTS); test mixture 6: t_0, uridine (U), N,N,N-trimethylphenylammonium chloride (TMPAC); test mixture 7: t_0, theobromine (Tb), theophylline (Tp).

2.2.2. Oligonucleotide samples

100-µM oligonucleotide aliquots were initially prepared by reconstituting lyophilized material in the appropriate volume of RNase-free water and stored at − 20 °C (DNA oligonucleotides) or − 80 °C (RNA oligonucleotides). Equimolar oligonucleotide mixtures were prepared by mixing aliquots and diluting the oligonucleotide products to 5 µM in RNase-free water or 10:90 H_2O/ACN prior to IP-RPLC or HILIC analysis, respectively. Volanesorsen is a fully phosphorothioated (PS) 20-mer antisense oligonucleotide containing ten MOE sugar moieties modifications and five 5-methylcytosines, having the following sequence A*G*mC*T*T*mC*T*T*G*T*mC*mC*A*G*mC*T*T*T*A*T (with * denoting PS linkage, mC for 5-methylcytosine, and underlined nucleotides containing the MOE). The chemical synthesis of this sample was hindered by the inclusion of the nt containing the 3 modifications simultaneously (mC*), therefore a sample missing the methylation on this specific nt (C* instead of mC*) was finally chosen for the study and referred to as vola henceforth in the text. Vola (reference) and derived oligonucleotide samples were prepared by diluting the oligonucleotide material to 2.5 µM in RNase-free water or 10:90 H_2O/ACN prior to IP-RPLC or HILIC analysis, respectively. Table 1 lists the investigated oligonucleotides and their characteristics.

2.3. Instrumentation and columns

Analyses were performed on an ACQUITY UPLC I-Class system (Waters, Milford, MA, USA), equipped with an auto-sampler including a 15-µL flow-through-needle (FTN) injector, a binary solvent delivery pump and a tunable ultraviolet (TUV) detector with a 500-nL analytical flow cell (10 mm path length). Absorbance data were acquired at 260 nm. Data acquisition and instrument control were performed by Empower 3 software (Waters). Table 2 lists the chromatographic columns investigated in this work while Fig. S1 represents the structures of the stationary phases. Of note, all columns were brand-new and shared the same sample history.

2.4. Chromatographic conditions

2.4.1. Gradient conditions for Tanaka test

Mobile phase was composed of a mixture of 90:10 acetonitrile and 20 mM ammonium acetate solution, pH 4.7 adjusted with acetic acid. The flow rate was set at 0.5 mL/min and column temperature was set at 30 °C. Isocratic separations were performed with compounds at 1 mg/mL, mixtures at 0.33 mg/mL and injection volume of 0.5 µL.

2.4.2. Gradient conditions for standard oligonucleotide mixtures

Mobile phases for IP-RPLC analyses were composed of 14 mM TEA, 160 mM HFIP in water, pH 8.1 (mobile phase A) and a mixture of 50:50 mobile phase A and methanol (mobile phase B). The flow rate was set at 0.3 mL/min and the column temperature at 60 °C. Gradients were adapted to the samples as retention can be very different based on the length of the oligonucleotides, therefore, a

Table 1
List of investigated oligonucleotides reporting short name, number of bases, sequence, molecular weight (MW), and modification type of each oligonucleotide. In the sequence, phosphorothioate (PS) linkages are indicated by a *, 2′-*O*-methoxyethyl modifications (MOE) by a _, and 5-methylcytosine modifications (5mC) by a *m*.

Short name	Bases	Sequence (5′-3′)	MW (g.mol^{-1})	Modifications
dT15–35 (equimolar mixture of dT15, dT20, dT25, dT30, and dT35)	15	TTT (TTT)$_{3}$ TTT	4500.9	Not modified
	20	TTT (TTT)$_{5}$ TT	6021.9	
	25	TTT (TTT)$_{7}$ T	7542.9	
	30	TTT (TTT)$_{8}$ TTT	9063.8	
	35	TTT (TTT)$_{10}$ TT	10584.8	
dT40–100 (equimolar mixture of dT40, dT60, dT80, dT100)	40	TTT (TTT)$_{12}$ T	12105.6 18189.8	Not modified
	60	TTT (TTT)$_{18}$ TTT	24273.7 30357.6	
	80	TTT (TTT)$_{25}$ TT		
	100	TTT (TTT)$_{32}$ T		
rU15–30 (equimolar mixture of rU15, rU20, rU30)	15	UUU (UUU)$_{3}$ UUU	4530.6	Not modified
	20	UUU (UUU)$_{5}$ UU	6061.4	
	30	UUU (UUU)$_{8}$ UUU	9123.1	
vola (reference)	20	$\underline{\mathrm{A^*G^*C^*T^*T}}^*\mathrm{mC^*T^*T^*G^*T^*mC^*mC^*A^*G^*mC^*}\underline{\mathrm{T^*T^*T^*A^*T}}$	7165.3	PS (19) MOE (10) mC (4)
vola-18mer	18	$\underline{\mathrm{C^*T^*T}}^*\mathrm{mC^*T^*T^*G^*T^*mC^*mC^*A^*G^*mC^*}\underline{\mathrm{T^*T^*T^*A^*T}}$	6342.5	PS (17) MOE (8) mC (4)
vola-19mer	19	$\underline{\mathrm{G^*C^*T^*T}}^*\mathrm{mC^*T^*T^*G^*T^*mC^*mC^*A^*G^*mC^*}\underline{\mathrm{T^*T^*T^*A^*T}}$	6761.9	PS (18) MOE (9) mC (4)
vola-22mer	22	$\underline{\mathrm{A^*A^*A^*G^*C^*T^*T}}^*\mathrm{mC^*T^*T^*G^*T^*mC^*mC^*A^*G^*mC^*}\underline{\mathrm{T^*T^*T^*A^*T}}$	7972.0	PS (21) MOE (12) mC (4)
vola-21mer	21	$\underline{\mathrm{A^*A^*G^*C^*T^*T}}^*\mathrm{mC^*T^*T^*G^*T^*mC^*mC^*A^*G^*mC^*}\underline{\mathrm{T^*T^*T^*A^*T}}$	7568.6	PS (20) MOE (11) mC (4)
Vola-18PS	20	$\underline{\mathrm{AG^*C^*T^*T}}^*\mathrm{mC^*T^*T^*G^*T^*mC^*mC^*A^*G^*mC^*}\underline{\mathrm{T^*T^*T^*A^*T}}$	7149.2	PS (18) MOE (10) mC (4)
Vola-17PS	20	$\underline{\mathrm{AGC^*T^*T}}^*\mathrm{mC^*T^*T^*G^*T^*mC^*mC^*A^*G^*mC^*}\underline{\mathrm{T^*T^*T^*A^*T}}$	7133.1	PS (17) MOE (10) mC (4)
vola-9MOE	20	$\mathrm{A^*}\underline{\mathrm{G^*C^*T^*T}}^*\mathrm{mC^*T^*T^*G^*T^*mC^*mC^*A^*G^*mC^*}\underline{\mathrm{T^*T^*T^*A^*T}}$	7091.2	PS (19) MOE (9) mC (4)
vola-8MOE	20	$\mathrm{A^*G^*}\underline{\mathrm{C^*T^*T}}^*\mathrm{mC^*T^*T^*G^*T^*mC^*mC^*A^*G^*mC^*}\underline{\mathrm{T^*T^*T^*A^*T}}$	7017.1	PS (19) MOE (8) mC (4)
vola-3mC	20	$\underline{\mathrm{A^*G^*C^*T^*T}}^*\mathrm{C^*T^*T^*G^*T^*mC^*mC^*A^*G^*mC^*}\underline{\mathrm{T^*T^*T^*A^*T}}$	7151.2	PS (19) MOE (10) mC (3)
vola-2mC	20	$\underline{\mathrm{A^*G^*C^*T^*T}}^*\mathrm{C^*T^*T^*G^*T^*C^*mC^*A^*G^*mC^*}\underline{\mathrm{T^*T^*T^*A^*T}}$	7137.2	PS (19) MOE (10) mC (2)
vola-1mC	20	$\underline{\mathrm{A^*G^*C^*T^*T}}^*\mathrm{C^*T^*T^*G^*T^*C^*C^*A^*G^*mC^*}\underline{\mathrm{T^*T^*T^*A^*T}}$	7123.2	PS (19) MOE (10) mC (1)
vola-0mC	20	$\underline{\mathrm{A^*G^*C^*T^*T}}^*\mathrm{C^*T^*T^*G^*T^*C^*C^*A^*G^*C^*}\underline{\mathrm{T^*T^*T^*A^*T}}$	7109.1	PS (19) MOE (10)

gradient of 20–60%B in 10 min was used for dT15–35 and rU15-30, while 30–70%B in 15 min was used for dT40–100.

Mobile phases for HILIC analyses were composed of 50 mM ammonium acetate in water, pH 6.9 (mobile phase A, no adjustment of pH) and acetonitrile (mobile phase B). The flow rate was set at 0.2 mL/min for ZIC-pHILIC column and 0.3 mL/min for the other columns. The column temperature was set at 40 °C. For Syncronis HILIC, Nucleodur HILIC and Nucleoshell HILIC columns, a gradient of 70–50%B in 10 min was used for dT15–35 and rU15–30, while a gradient of 65–45%B in 15 min was used for dT40–100. For OH5 and HILIC-Z columns, a gradient of 65–45%B in 10 min was used for dT15–35 and rU15–30, while a gradient of 60–40%B in 15 min was used for dT40–100. For ZIC-pHILIC, gradients of 60–40%B in 22.5 min, 55–35%B in 22.5 min and 55–35%B in 34 min were used for dT15–35, rU15–30 and dT40–100, respectively. For Amide and ZIC-cHILIC columns, a gradient of 55–35%B in 10 and 15 min, respectively was used for dT15–35 and rU15–30, while a gradient of 50–30%B in respectively 15 and 22.5 min was used for dT40–100. Elution was not achieved using the Z-HILIC column: the tested gradient was 70–10%B followed by a 1-min washing step at 10%B. A reversed gradient of 10–70%B washed out the oligonucleotides.

Oligonucleotides were concentrated at 5 µM in each mixture and injection volume was 1 µL. Gradient conditions were optimized during preliminary studies. All gradients were systematically followed by an 8-min re-equilibration step performed at the initial gradient conditions.

2.4.3. Chromatographic conditions for highly modified oligonucleotides

Mobile phases for IP-RPLC analyses were composed of 14 mM TEA, 160 mM HFIP in water, pH 8.1 (mobile phase A) and a mixture of 50:50 mobile phase A and methanol (mobile phase B). The flow rate was set at 0.3 mL/min and the column temperature at 60 °C. For all modified oligonucleotides evaluated in IP-RPLC mode, a gradient of 40–60%B in 10 min was used.

Mobile phases for HILIC analyses were composed of 50 mM ammonium acetate in water, pH 6.9 (mobile phase A, no adjustment of pH) and acetonitrile (mobile phase B). The flow rate was set at

Table 2
List of investigated chromatographic columns and their properties.

Short name	Mode	Name	Manufacturer	Surface chemistry	Particle type	Column Hardware	Column dimensions (mm)	Particle size (µm)	Pore size (Å)
C18	IP-RP	Acquity Premier Oligonucleotide BEH C18	Waters	C18	Ethylene-bridged hybrid organic-inorganic particles	MaxPeak™ High Performance Surfaces	100 × 2.1	1.7	130
Amide	HILIC	Acquity Premier BEH Amide	Waters	Amide	Ethylene-bridged hybrid organic-inorganic particles	MaxPeak™ High Performance Surfaces	100 × 2.1	1.7	130
OH5		InfinityLab Poroshell 120 HILIC-OH5	Agilent	Poly-hydroxy fructan	Core-shell silica particles	Stainless-steel	100 × 2.1	2.7	120
Z-HILIC		Atlantis Premier BEH Z-HILIC	Waters	Zwitterion (sulfobetaine)	Ethylene-bridged hybrid organic-inorganic particles	MaxPeak™ High Performance Surfaces	100 × 2.1	1.7	95
ZIC-cHILIC		SeQuant ZIC-cHILIC	Merck	Zwitterion (phosphorylcholine)	Fully-porous silica particles	PEEK-lined stainless-steel (Titanium frits)	150 × 2.1	3	100
ZIC-pHILIC		SeQuant ZIC-pHILIC	Merck	Zwitterion (sulfobetaine)	Porous polymer beads	PEEK-lined stainless-steel (Titanium frits)	150 × 2.1	5	n.a.
Nucleodur HILIC		Nucleodur HILIC	Macherey-Nagel	Zwitterion (sulfobetaine)	Fully-porous silica particles	Stainless-steel	50 × 2	1.8	110
Nucleoshell HILIC		Nucleoshell HILIC	Macherey-Nagel	Zwitterion (sulfobetaine)	Core-shell silica particles	Stainless-steel	100 × 3	2.7	90
HILIC-Z		InfinityLab Poroshell 120 HILIC-Z	Agilent	Zwitterion (sulfobetaine)	Core-shell silica particles	PEEK-lined stainless-steel	100 × 2.1	2.7	100
Syncronis HILIC		Syncronis HILIC	Thermo Scientific	Zwitterion (sulfobetaine)	Fully-porous silica particles	Stainless-steel	100 × 2.1	1.7	100

0.2 mL/min for ZIC-pHILIC column (due to limited mechanical stability) and 0.3 mL/min for the other columns. The column temperature was set at 40 °C. For Syncronis HILIC and Nucleodur HILIC columns, a gradient of 72–62%B in 10 and 5 min was used, respectively. For OH5 and HILIC-Z columns, a gradient of 65–55%B in 10 min was used. For Amide column, a gradient of 60–50%B in 10 min was used. For ZIC-cHILIC column, a gradient of 55–45%B in 15 min was used.

Oligonucleotides were concentrated at 2.5 µM in each mixture and injection volume was 1 µL. Gradient conditions were optimized during preliminary studies. All gradients were systematically followed by an 8-min re-equilibration step performed at the initial gradient conditions.

2.5. Chromatographic descriptors

The composition at elution, $C_{e,}$ was determined according to the following equation:

$$C_e = C_i + \frac{C_f - C_i}{t_G}(t_r - t_0 - t_D)$$

where C_i and C_f are the initial and final mobile phase compositions (%), respectively, t_G the gradient time (min), t_R the retention time (min) and t_D the dwell time (min). The dwell time was estimated by dividing the dwell volume, 100 µL, by the flow rate (µL/min).

Peak capacity, P, was calculated using the average peak width at 50% ($w_{50\%}$) and determined according to the following equation:

$$P = 1 + \frac{t_G}{1.7 \times w_{50\%}}$$

3. Results and discussion

3.1. Tanaka test for highlighting the main attributes of the investigated columns

As zwitterionic HILIC columns have shown interest for the analysis of oligonucleotides, several zwitterionic HILIC stationary phases were selected for our comparison study [13]. This included six sulfobetaine stationary phases from different manufacturers (*i.e.* Z-HILIC from Waters, ZIC-pHILIC from Merck, Nucleodur HILIC and Nucleoshell HILIC from Macherey-Nagel, HILIC-Z from Agilent and Syncronis HILIC from Thermo Fisher Scientific) and one phosphorylcholine stationary phase from Merck (ZIC-cHILIC). Both OH5 and Amide columns (from Agilent and Waters, respectively) were also added to the study as HILIC reference materials. Detailed information about the investigated columns is available in Table 1. To properly compare column characteristics and highlight their differences, the well-accepted test scheme for HILIC columns (also called Tanaka test) was performed [20]. As described by Kawachi et al., a mobile phase containing 90:10 ACN/20 mM aqueous ammonium acetate was used, and thirteen analytes were injected separately and as mixtures on each column to interrogate different types of selectivity.

However, it is important to keep in mind that the Tanaka test utilized small molecule analytes that are very different from oligonucleotides in terms of structure and complexity. This test was a first indicator of the retention and selectivity behavior of HILIC columns, but further investigation had to be performed with oligonucleotides (Section 3.2).

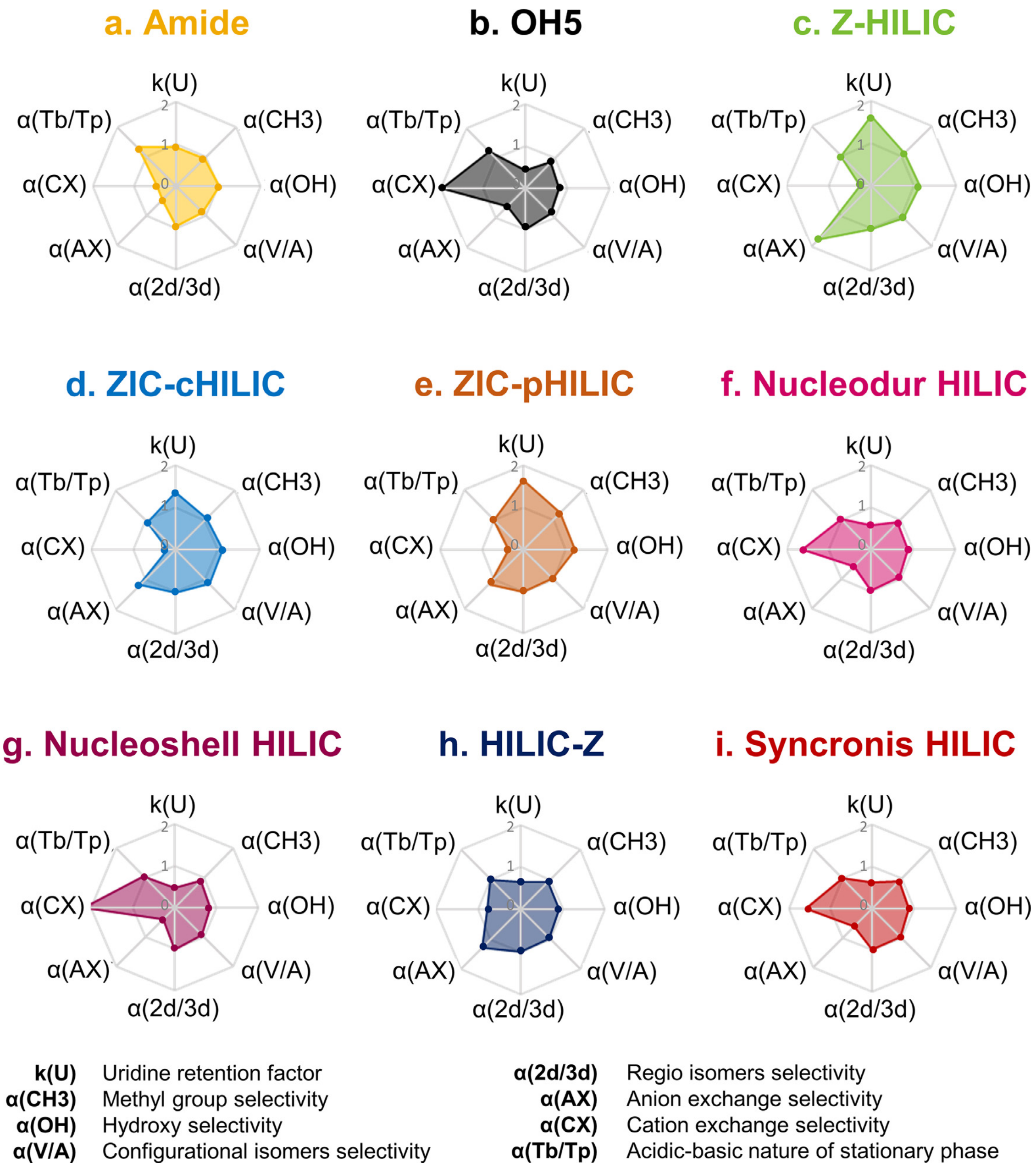

Fig. 1. Tanaka test: Radar plots of HILIC stationary phases. Each parameter was normalized by setting each average value for zwitterionic columns to 1.0, to discriminate columns based on their comparison to the average responses of zwitterionic columns. Normalized data are reported in Table S1, while average values and raw data are reported in Table S2 and Table S3, respectively.

Based on relative retention of key analyte pairs, different selectivity values were calculated: relative retention of 5-methyluridine *vs.* uridine (U) for methyl group selectivity (α(CH$_3$)), relative retention of uridine *vs.* 2′-deoxyuridine for hydroxy selectivity (α(OH)), relative retention of adenosine *vs.* vidarabine for configurational isomers selectivity (α(V/A)), relative retention of 2′-deoxyguanosine *vs.* 3′-deoxyguanosine for regio isomers selectivity (α(2d/3d)), relative retention of sodium *p*-toluenesulfonate *vs.* uridine for anion exchange selectivity (α(AX)), relative retention of N,N,N-trimethylphenylammonium *vs.* uridine for cation exchange selectivity (α(CX)), relative retention of theobromine *vs.* theophylline for surface acidity (α(Tb/Tp)), in addition to the retention factor of uridine (k(U)).

For each parameter, the average response of the zwitterionic columns was taken as the reference value (1) to obtain normalized values for each HILIC column. Normalized data for each column have been reported in Table S1 and summarized in Fig. 1 as radar-shaped representations. Non-normalized values for each parameter and corresponding raw data were reported in Tables S2 and S3, respectively.

First, surface acidity of stationary phases was measured from the relative retention of theobromine *vs.* theophylline, with the highest α(Tb/Tp) values showing greatest local acidity. As expected, no selectivity between these two xanthine derivatives was observed for most zwitterionic columns, being neutral stationary phases, even if Nucleoshell HILIC and ZIC-cHILIC columns resulted in little selectivity. This could be traced back by the order of the charged groups at the phase surface. Despite the 1:1 ratio of oppositely charged functional groups of zwitterionic columns, sulfobetaine phases such as Nucleoshell HILIC exhibit negatively charged sulfonic groups at the outer surface, that give a slightly acidic nature to the stationary phase surface. Conversely, positively charged choline groups of the ZIC-cHILIC column (oriented at the end of the zwitterionic groups) give a slightly basic nature to the stationary phase surface. Acidic nature of amide and OH5 stationary phases have also been reported with α(Tb/Tp) values of 1.22 and 1.30 (Table S2).

Based on the retention factor of uridine (k(U)), hydrophilicity and therefore retentivity of HILIC stationary phases can also be estimated. With normalized k(U) values (k^N(U)) comprised between 1.37 and 1.65, ZIC-cHILIC, ZIC-pHILIC and Z-HILIC columns were among the most retentive materials with greater hydrophilic interactions of uridine with zwitterionic phases.

Besides polar interactions, hydrophilic partitioning contributes to the HILIC mechanism. Indeed, it was found that α(OH) can be used to estimate the thickness of the adsorbed water layer and thus represents partitioning [21]. In any case, α(OH) values were greater than 1, with the greatest values for Z-HILIC, ZIC-cHILIC and ZIC-pHILIC columns (Table S2). It highlights selectivity towards hydrophilic groups, which is an important parameter to separate DNA *vs.* RNA oligonucleotides that differ by hydroxy moieties, for instance. Despite having hydroxy selectivity, small differences were observed between columns, with maximum 22% deviation from the average response ($0.80<\alpha^N(\mathrm{OH})<1.22$). Therefore, this selectivity parameter cannot be used to discriminate columns based on their ability to partition.

Finally, as polar molecules are often ionic, electrostatic interactions also participate to the overall retention mechanism in HILIC. Interestingly, our results confirmed that one cannot characterize stationary phases by low or high ion-exchange interactions based on their functionalization, but some trends were still observed [22]

First, HILIC columns can be classified by their cation-exchange (CX) activity expressed by α(CX) values, with ZIC-cHILIC showing the smallest CX activity with an α(CX) value of 0.37. Due to the relation between ion-exchange capabilities and surface acidity, we can say that the exposed sulfonic groups at the surface of sulfobetaine phases induce their CX retention behavior, contrary to the negative charge of the phosphorylcholine group (ZIC-cHILIC) that is not exposed. CX phenomenon can also be enhanced in the presence of residual silanols functionality, and can therefore be mitigated for hybrid silica particles whose silanol activity is reduced [23–25]. This was confirmed by the low α^N(CX) values for these columns (0.47 for Amide, 0.26 for Z-HILIC, Table S1).

In the case of oligonucleotides, that are negatively charged compounds, CX interactions contribute to a lesser extent to the overall retention mechanism as opposed to anion exchange (AX) interactions. Therefore, besides k(U), α(AX) is also an important parameter to consider for explaining retention and selectivity of anionic compounds. Z-HILIC, HILIC-Z, ZIC-cHILIC, and ZIC-pHILIC columns resulted in the highest AX selectivities with α^N(AX) values of 1.77, 1.28, 1.18, and 1.17, respectively (Table S1). Compared to these columns, other columns have moderate to low AX capacities.

Then, based on the k(U) and α(AX) values, columns may be categorized by their relative ability to retain negatively charged analytes. Z-HILIC, ZIC-pHILIC, ZIC-cHILIC are expected to be the most retentive materials, followed by HILIC-Z, and finally Amide, Syncronis HILIC, Nucleodur HILIC, OH5, and Nucleoshell HILIC columns that should be the less retentive materials.

The results also showed that other selectivity parameters exist and may interfere in the global selectivity behavior of the HILIC columns. The relative retention of 5-methyluridine and uridine ($\alpha(\mathrm{CH_3})$) is a measure of the methyl group selectivity and provides information on the hydrophobic character of the stationary phases that is needed to discriminate a methylated impurity to its original oligonucleotide, for instance. Based on this test, selectivity for hydrophobic groups was observed for all columns with $\alpha(\mathrm{CH_3})$ values greater than 1 (Table S2). Again, Z-HILIC, ZIC-cHILIC and ZIC-pHILIC columns proved to have the highest $\alpha(\mathrm{CH_3})$ values, but little differences between columns were observed (deviation of 22% from the average value). ZIC-cHILIC also exhibited better configurational and regio isomers selectivities (α(V/A) and α(2d/3d)) than the other columns. Finally, if we look at the overall selectivity profile given by radar plots (Fig. 1), some columns showed very similar chromatographic behavior. A high degree of similarity was indeed observed between Nucleodur HILIC and Nucleoshell HILIC (both from Macherey-Nagel). This was expected as they only differ by their particle morphology, having fully-porous *vs.* core-shell particles. Syncronis HILIC was also found to be very similar to Macherey-Nagel columns. ZIC-pHILIC and ZIC-cHILIC also exhibited quite close selectivity properties. Slightly higher selectivities were obtained for ZIC-cHILIC in terms of isomers selectivity and anion exchange selectivity (1.67 *vs.* 1.42, 0.37 *vs.* 0.36, respectively). ZIC-pHILIC offered better selectivities in terms of cation exchange interactions, methyl group and hydroxy group selectivities (0.80 *vs.* 0.37, 1.69 *vs.* 1.47, 2.03 *vs.* 1.90, respectively). On the other hand, retention and selectivity behavior of the HILIC-Z column were found to be very close to the average response provided by the other zwitterionic columns.

3.2. Evaluation of the zwitterionic columns with model ONs

Next to the evaluation of various HILIC stationary phases with small molecules, these columns were also tested with model oligonucleotides composed of 15 to 100 nucleobases, corresponding to molecular weights in the range of 4′500 to 30′000 Da. Both model DNA (poly-deoxythymidylic acid sequence, dT) and RNA (poly-uridylic acid sequence, dU) oligonucleotides were tested. The corresponding chromatograms have been reported in Fig. 2 (dT15-35 mixture), Fig. 3 (dT40-100 mixture) and Fig. S2 (rU15–30 mixture). The data obtained with the different zwitterionic stationary phases (*i.e.* Z-HILIC, ZIC-cHILIC, ZIC-pHILIC, Nucleodur HILIC, Nucleoshell HILIC, HILIC-Z and Syncronis HILIC) were systematically compared with two other reference HILIC chemistries (Amide and OH5), and also a C18 column used under IP-RPLC conditions. All the figures of merit obtained for the different mixtures of DNA and RNA ONs on these 10 different columns were summarized in Table 3.

3.2.1. Evaluation with model DNA ONs: dT15 to dT35

Fig. 2 shows the chromatograms obtained for the mixture composed of dT15, dT20, dT25, dT30 and dT35 (five peaks). As illustrated, the different dT species can be eluted under all conditions, except on the Z-HILIC, which was found to be too retentive for this sample. As highlighted in Section 3.1, this behavior can be attributed to its high ion exchange character α(AX) and important hydrophilicity k(U), which are both responsible for the retention of ONs. The Z-HILIC column was able to analyze the small model molecules (Tanaka test) but was unsuitable for large ONs possessing a significant number of polar groups and negative charges. As reported in Table 3, three figures of merit were considered to compare the remaining nine columns, namely the composition at elution for dT20 (C_e), the selectivity (α) between dT15 and dT20, and the peak capacity (P, calculated by considering the peak widths of the five most intense peaks).

In terms of retention, the less retentive HILIC stationary phases were the Nucleodur HILIC (highest C_e of 63.6%ACN), the Syncronis HILIC (C_e of 61.6%ACN), and the Nucleoshell HILIC (C_e of 59.4%ACN). On the contrary, the most retentive columns were the Amide (lowest C_e of 43.9%ACN), the ZIC-cHILIC (C_e of 45.8%ACN), and the ZIC-pHILIC (C_e of 47.9%ACN). The remaining two HILIC columns (OH5 and HILIC-Z) showed an intermediate retention behavior. Except for the Amide and OH5 columns that were more re-

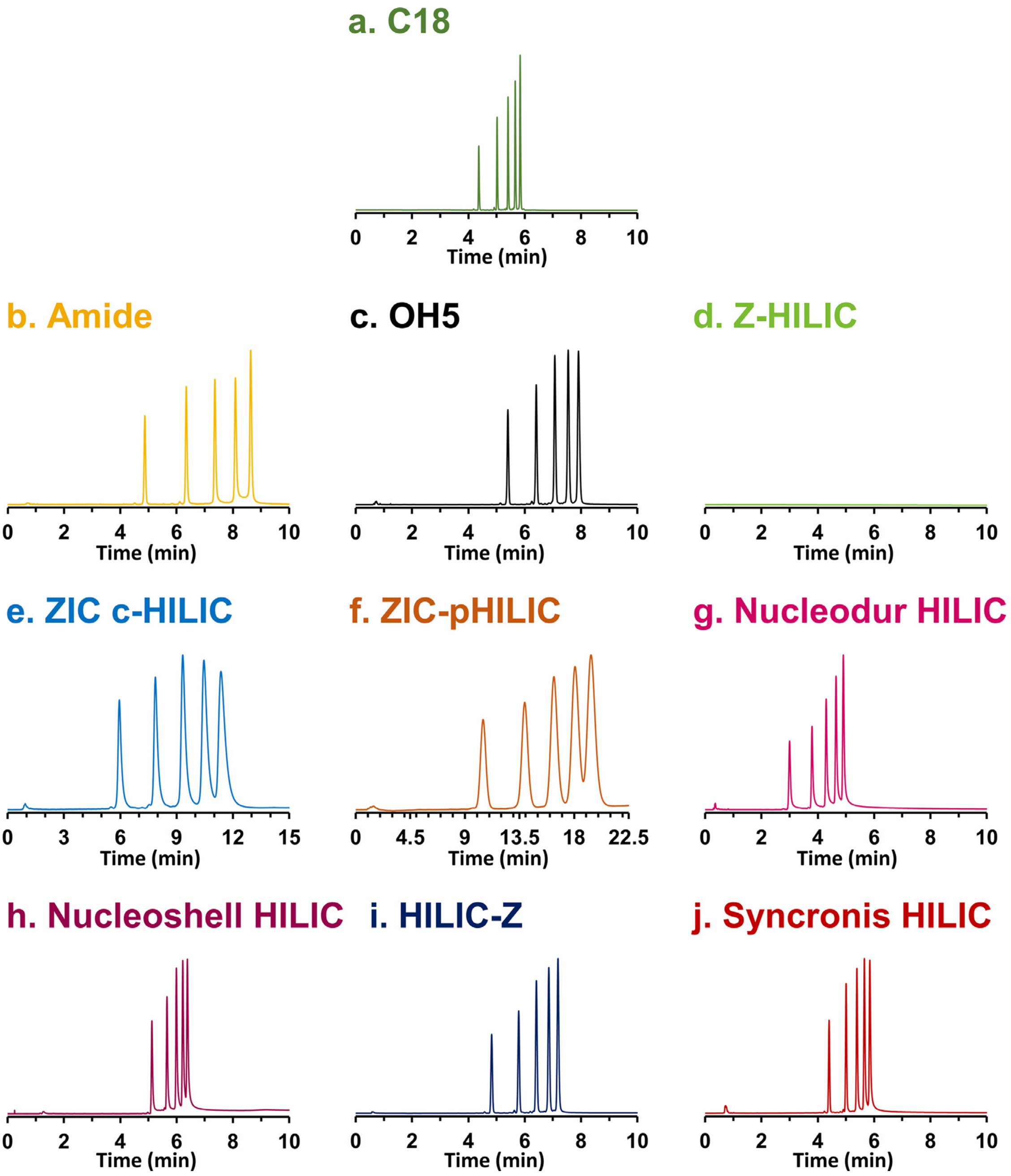

Fig. 2. Chromatograms of dT15–35 mixture obtained by using the C18 column (a), the amide column (b), the OH5 column (c) and the zwitterionic columns (d – j). For chromatographic conditions and specifications on the columns, please refer to Section 2.4.2 and Table 2, respectively.

Table 3
For each column, chromatographic descriptors for standard ON mixtures are reported, namely % of organic mobile phase composition at the elution (C_e) for dT20, dT60 and rU20; selectivities between dT15/dT20, dT40/dT60 and rU15/rU20 (α); and peak capacities for each mixture (P, calculated using the average peak width @50%). Corresponding chromatograms are provided in Fig. 2 (dT15–35 mixture), Fig. 3 (dT40–100 mixture) and Fig. S2 (rU15–30 mixture).

	Descriptors	C18	Amide	OH5	ZIC-cHILIC	ZIC-pHILIC	Nucleodur HILIC	Nucleoshell HILIC	HILIC-Z	Syncronis HILIC
	t_0	0.810	0.470	0.451	0.630	0.571	0.237	0.813	0.411	0.484
Descriptors for dT15–35	C_e (%) for dT20	35.5	43.9	53.8	45.8	47.9	63.6	59.4	54.9	61.6
	α(dT15/dT20)	1.18	1.33	1.20	1.36	1.35	1.29	1.12	1.22	1.15
	P	197	94	94	35	23	107	126	102	131
Descriptors for dT40–100	C_e (%) for dT60	35.2	37.8	49.7	38.2	41.1	61.0	58.9	51.7	59.9
	α(dT40/dT60)	1.13	1.22	1.20	1.33	1.22	1.38	1.17	1.18	1.18
	P	140	70	54	20*	20**	108	122	88	116
Descriptors for rU15–30	C_e (%) for rU20	26.4	38.2	53.1	42.0	34.7	62.3	58.2	53.3	60.5
	α(rU15/rU20)	1.54	1.21	1.19	1.27	1.20	1.21	1.11	1.17	1.13
	P	215	91	97	33	26***	96	109	99	113

* Based on dT40 only (wdT60 to wdT100 could not be calculated)

** Based on dT40 and dT60 only (w^{dT80} and w^{dT100} could not be calculated)

*** Based on rU15 only (w^{rU20} to w^{rU30} could not be calculated)

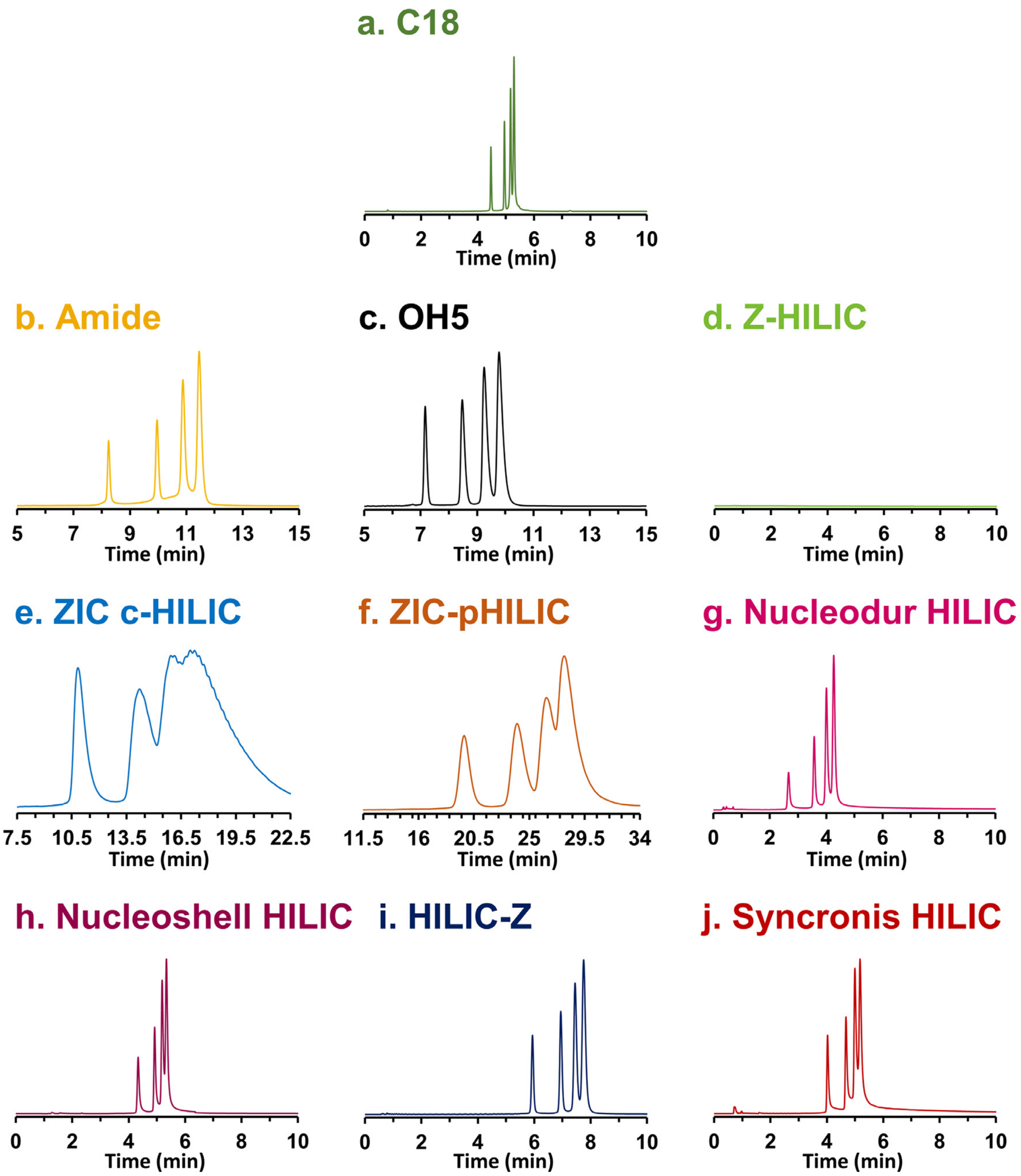

Fig. 3. Chromatograms of dT40–100 mixture obtained by using the C18 column (a), the amide column (b), the OH5 column (c) and the zwitterionic columns (d – j). For chromatographic conditions and specifications on the columns, please refer to Section 2.4.2 and Table 2, respectively.

tentive than expected, these results are in line with the observations made in Fig. 1 with small molecules for k(U) and α(AX), as these are the two most important features to explain the retention of ONs (negatively charged, polar molecules).

In terms of selectivity between dT15 and dT20, the best results were obtained for the three most retentive stationary phases (Amide, ZIC-pHILIC and ZIC-cHILIC with α between 1.33 and 1.36), while the lowest selectivity values were reached for the two columns providing intermediate retention (OH5 and HILIC-Z, with α between 1.20 and 1.22). Interestingly, selectivity was generally better in HILIC *vs*. IP-RPLC (α of only 1.18), whatever the HILIC column employed. Finally, only the ZIC-cHILIC and ZIC-pHILIC offered higher selectivity than the reference HILIC material (Amide).

Next, peak capacity was also evaluated for the different stationary phases. To have comparable results among all the tested conditions, it is important to notice that the gradient was always adjusted to the column dimensions (geometrical scaling of the gradient between columns of different lengths). IP-RPLC with C18 column packed with fully porous 1.7 µm particles largely outperformed the HILIC conditions, with a P value of 197. In the case of HILIC conditions, peak capacity was between 94 and 131, except for the ZIC-cHILIC and ZIC-pHILIC, which offered a P value of only 35 and 23, respectively. This behavior is clearly visible in Fig. 2, where the dT peaks are much broader on these two columns compared to the other conditions. This performance can be due to the fact that these columns are packed with 3 or 5 µm fully porous particles, therefore offering limited kinetic performance. An additional restriction of the ZIC-pHILIC is its limited mechanical stability (upper pressure limit of only 200 bar), due to its polymeric nature. Remarkably, the two non-zwitterionic columns (Amide and

OH5) offered a peak capacity of only 94, which was also quite low compared to the Nucleoshell HILIC (P = 126) and Syncronis HILIC (P = 131). The very good peak capacity obtained on the Nucleoshell HILIC can be attributed to the particle morphology (core-shell type particles of 2.7 µm). However, the OH5 and HILIC-Z, also composed of core-shell particles, and the Syncronis HILIC made of fully-porous particles, do not offer the same level of performance.

Finally, despite the higher selectivity observed on the ZIC-cHILIC and ZIC-pHILIC columns, the overall resolution was unsatisfactory on these two columns, due to the low kinetic performance. The best resolution was achieved on the Amide column under HILIC conditions (high selectivity and reasonable peak capacity), while the resolution obtained under IP-RPLC mode with the C18 column was lower (excellent peak capacity, but limited selectivity). Among the zwitterionic stationary phases, the HILIC-Z and Nucleodur HILIC were found to be the most promising ones.

3.2.2. Evaluation with model DNA ONs: dT40 to dT100

Fig. 3 shows the chromatograms obtained for the mixture composed of dT40, dT60, dT80 and dT100 (four peaks). Here again, the Z-HILIC was found to be unsuitable for this sample (no elution of the different species). In terms of retention, the trends were exactly the same as for the dT15–35 mixture. This behavior is logical, as the chemical nature of the ONs was not changed, only the size was increased. However, the %ACN required to elute dT60 in HILIC conditions was in average 4% lower than the one required to elute dT20.

In the case of dT40 to dT100, selectivity was the lowest on the C18 column under IP-RPLC mode (α was equal to 1.13 between dT40 and dT60), while it was the highest on the Nucleodur HILIC ($\alpha = 1.38$) and ZIC-cHILIC ($\alpha = 1.33$). The six remaining HILIC columns showed very close selectivity values comprised at an intermediate level, between 1.17 and 1.22.

Last, peak capacities were also evaluated, and values ranged between 20 and 140. The ZIC-cHILIC and ZIC-pHILIC offered the lowest peak capacity and were clearly not adapted for the analysis of large ONs, as illustrated in Fig. 3e-f, where very broad peaks were observed. The amide and OH5 stationary phases also possess a limited peak capacity of 70 and 54, respectively. Here again, the C18 operating under IP-RPLC mode provided the highest P value of 140, but two zwitterionic HILIC columns (*i.e.* Nucleoshell HILIC and Syncronis HILIC) were quite close, with P of 116 and 122. Surprisingly, we found no direct correlation between peak capacity and pore size, despite the fact that the dT40 to dT100 have molecular weights comprised between 12 and 30 kDa. Indeed, for the tested columns, pore size varies from 90 to 130 Å, but the largest pores do not give necessarily the highest peak capacity. However, the differences in pore sizes were quite minor, and it would be interesting to test much larger pore sizes of 300 to 1000 Å with these large ONs, to evaluate the real impact of pore size on kinetic performance [26]

For larger ONs, HILIC mode allowed to obtain much better overall resolution compared to IP-RPLC, as reported in Fig. 3. The Z-HILIC, ZIC-cHILIC, and ZIC-pHILIC columns were clearly unsuitable for the analysis of such large ONs. However, other zwitterionic HILIC columns were found to be particularly promising. Indeed, compared to the amide and OH5 HILIC phases, zwitterionic HILIC columns (Nucleodur HILIC, Nucleoshell HILIC, HILIC-Z, and Syncronis HILIC) clearly offered higher peak capacities.

3.2.3. Evaluation with model RNA ONs: rU15 to rU30

Fig. S2 shows the separation of model RNA ONs (rU15, rU20, rU30) having sizes comprised between 4.5 and 9.1 kDa. The main difference between poly dT previously analyzed and poly rU analyzed in Fig. S2 lies in the presence of an additional hydroxyl group on the sugar unit for poly rU, in replacement of a hydrogen atom. In addition, an additional methyl group is located on the thymine *vs.* uracil. Also in this case, Z-HILIC was found to be unsuitable for the analysis of RNA ONs (no peak observed).

In terms of retention, the analytical conditions to elute rU20 required in average 4% more water in HILIC conditions compared to dT20. The ZIC-pHILIC was an outlier, much more retentive towards rU20, requiring at least 13% more water in the mobile phase, compared to dT20. The retention under IP-RPLC conditions was also quite different, with a reduction of ACN by 9% compared to dT20. The IP-RPLC behavior can be attributed to the presence of additional methyl groups on the dT *vs.* rU species, leading to stronger hydrophobic interactions, while the difference observed under HILIC conditions might be related to the presence of hydroxyl group on rU *vs.* dT, leading to more H-bonds and hydrophilic partitioning.

Besides retention, selectivity between rU15 and rU20 was also evaluated. Similarly to what was observed for dT15 and dT20, the selectivity was slightly lower for the Syncronis HILIC ($\alpha = 1.13$) and the Nucleoshell HILIC ($\alpha = 1.11$), compared to the other HILIC columns. All the other HILIC columns had very close selectivity values comprised between 1.17 and 1.27. This means that the presence of an additional hydroxyl group on the sugar moiety does not impact so much selectivity between rU species. On the other hand, the selectivity rU15/rU20 was much higher ($\alpha = 1.54$) under IP-RPLC (C18 column), and this was not the case for dT15/dT20. So, it appears that the presence of additional methyl groups is probably responsible for the higher selectivity due to more significant changes in hydrophobicity between rU species.

Finally, peak capacity was again very low for the ZIC-cHILIC and ZIC-pHILIC (P of 26 and 33, respectively), while it varied between 91 and 113 for the other HILIC stationary phases and was as high as 215 for IP-RPLC conditions. These results are quite comparable to what we observed for dT15-35 and can be attributed to the same reasons.

3.3. Evaluation of the zwitterionic columns with chemically modified 20-mer ONs

Next to the model DNA and RNA oligonucleotides of various lengths, we have focused our attention on chemically modified 20-mer ONs, which are far more representative of commercially available products [5]. The mobile phases employed in IP-RPLC and HILIC modes were strictly identical to Section 3.2. Three HILIC columns were discarded from the pool, namely the Z-HILIC that does not allow the elution of ONs, the ZIC-pHILIC that has a very similar behavior and always provides lower performance than the ZIC-cHILIC, and the Nucleoshell HILIC that provides comparable chromatographic behavior as the Nucleodur HILIC, but with lower selectivity. The gradient profiles were also adjusted case by case to systematically maximize performance. Table 1 describes the different ONs that were considered for this part of the work.

As reported in Table 1, our reference ON (vola) is quite complex, with several chemical modifications to improve drug-like properties, namely the presence of 19 phosphorothioate (PS) linkages instead of phosphodiester (PO) linkages, 10 different 2′-O-methoxyethyl (MOE) modifications on sugar units located at the beginning and the end of the sequence, and methylation of all the cytosine (mC), except the first one, as previously mentioned.

Different variants of this reference material were synthesized, having different lengths (number of nucleotides varying between 18 and 22), number of methylated cytosine (from 0 to 4), number of PS linkages (comprised between 17 and 21), and MOE modifications (ranging from 8 to 12). The goal was to assess whether IP-RPLC or HILIC conditions allow the separation of these different species with known modifications. All the corresponding chromatograms were reported in Fig. 4 (vola *vs.* ONs having different

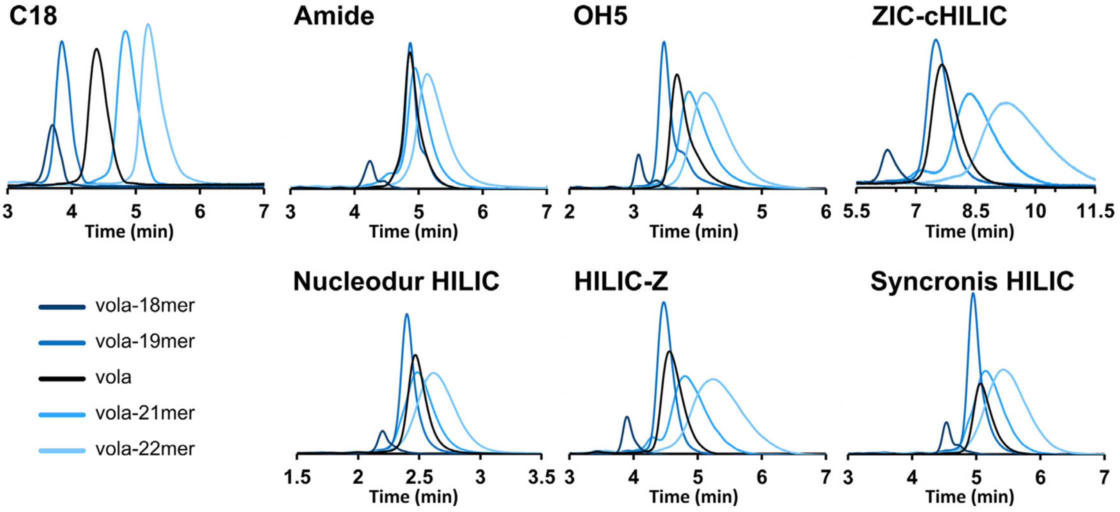

Fig. 4. Comparison of columns used for the analysis of vola (reference) and derived oligonucleotides that differ in terms of sequence length. Overlaid chromatograms obtained on C18 and 6 HILIC columns (1 amide, 1 OH5 and 4 zwitterionic columns, namely ZIC-cHILIC, Nucleodur HILIC, HILIC-Z, and Syncronis HILIC) related to vola-18mer (darkest blue trace), vola-19mer (dark blue trace), vola (black trace), vola-21mer (light blue trace), and vola-22mer (lightest blue trace).

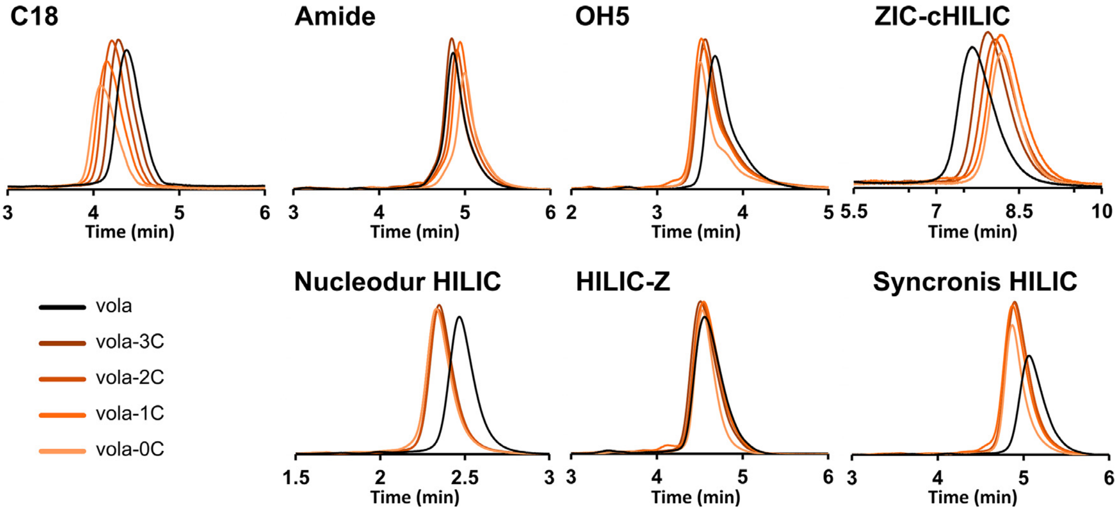

Fig. 5. Comparison of columns used for the analysis of vola (reference) and derived oligonucleotides that differ in terms of number of 5-methylcytosine modifications. Overlaid chromatograms obtained on C18 and 6 HILIC columns (1 amide, 1 OH5 and 4 zwitterionic columns, namely ZIC-cHILIC, Nucleodur HILIC, HILIC-Z, and Syncronis HILIC) related to vola (black trace), vola-3C (darkest gray trace), vola-2C (dark orange trace), vola-1C (orange trace), and vola-0C (light orange trace).

lengths), Fig. 5 (vola *vs.* ONs having different number of methylated cytosine), Fig. 6 (vola *vs.* ONs having different number of PS linkages), and Fig. 7 (vola *vs.* ONs having different number of MOE modifications), while the corresponding figures of merit were included in Table 4.

3.3.1. Analysis of ONs having different lengths

Fig. 4 shows the results obtained for the analysis of ONs having different lengths (number of nucleobases comprised between 18 and 22) with the seven different analytical conditions in IP-RPLC and HILIC modes. As illustrated, it appears that the C18 under IP-RPLC provided the best selectivity (in average α was equal to 1.19), which is not surprising, as this chromatographic mode has been found to be ideal to separate ONs of varying lengths, due to the addition of one TEA molecule *per* nucleotide, leading to enhanced hydrophobicity [27]. Besides this column, HILIC also showed comparable selectivity confirming its promising use for the separation of MOE modified oligonucleotides and their length-based impurities [13]. The ZIC-cHILIC provided a relatively good selectivity of 1.15 in average, while the amide column (current reference in HILIC mode) was the worst one ($\alpha = 1.06$ in average). Compared to previous experiments (Sections 3.1. and 3.2.), it is important to notice that the kinetic performance was strongly reduced, and average peak capacity varied from only 13 (ZIC-cHILIC) to 25 (Amide). These values are far from the ones obtained with model ONs (P up to 215 when using IP-RPLC, while the highest value using HILIC was only 131). The low P values can be explained by the presence of diastereoisomers (due to the presence of several PS linkages), and a partial diastereoisomeric separation [28]. Indeed, a partial separation of phosphorothioate oligonucleotide diastereoisomers resulted in wider peaks compared to phosphodiester oligonucleotides of the same sequence [29,30]

In the end, the ZIC-cHILIC was very promising in terms of selectivity but suffers from poor kinetic performance. Therefore, the C18 column under IP-RPLC mode remains the most suitable column to separate these congeneric species (*i.e.* n-2, n-1, n, n+1 and n+2).

3.3.2. Analysis of ONs having different number of methylated cytosine

Fig. 5 shows the separation of the different ON species having a number of mC comprised between 0 and 4. In this case, the separation was harder to achieve, as selectivity varied in average between 1.01 (HILIC-Z and Amide) and 1.06 (C18, ZIC-cHILIC and Nu-

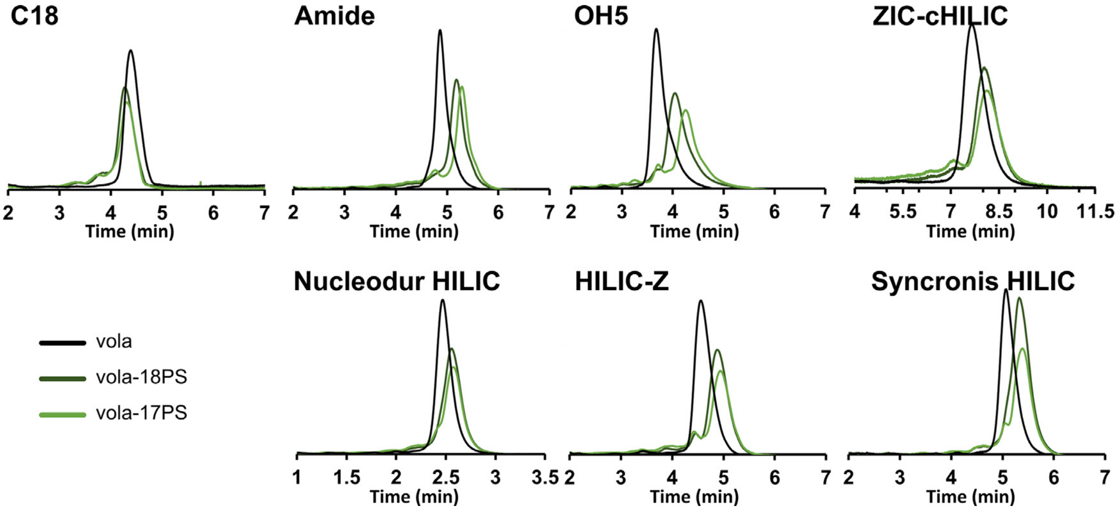

Fig. 6. Comparison of columns used for the analysis of vola (reference) and derived oligonucleotides that differ in terms of backbone composition (phosphodiester impurities). Overlaid chromatograms obtained on C18 and 6 HILIC columns (1 amide, 1 OH5 and 4 zwitterionic columns, namely ZIC-cHILIC, Nucleodur HILIC, HILIC-Z, and Syncronis HILIC) related to vola (black trace), vola-18PS (dark green), and vola-17PS (light green).

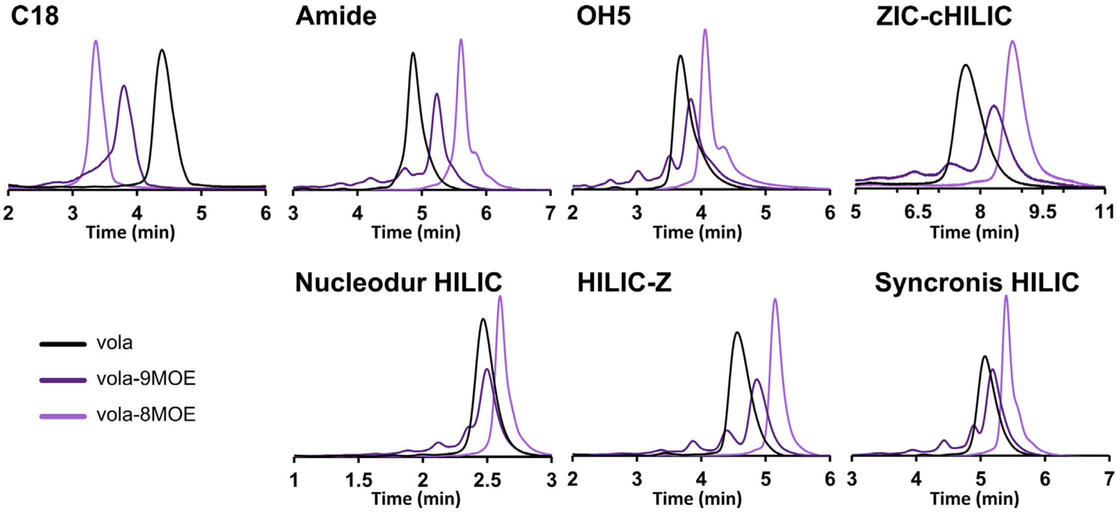

Fig. 7. Comparison of columns used for the analysis of vola (reference) and derived oligonucleotides that differ in terms of number of 2′-O-MOE modifications. Overlaid chromatograms obtained on C18 and 6 HILIC columns (1 amide, 1 OH5 and 4 zwitterionic columns, namely ZIC-cHILIC, Nucleodur HILIC, HILIC-Z, and Syncronis HILIC) related to vola (black trace), vola-9MOE (dark purple), and vola-8MOE (light purple).

cleodur HILIC). The only difference between the products was the addition of one or several methyl groups on the cytosine residues. The addition of a lipophilic group has obviously a very limited impact on the hydrophilic partitioning, so the HILIC behavior remains highly comparable between the five different species, and only the reference material with 4 mC was slightly separated from the other species. In IP-RPLC mode, a larger effect should be expected, as the hydrophobicity of the product is probably enhanced by the addition of one or several methyl groups. However, due to the steric hindrance and possible conformational changes (folding), it is possible that this additional methyl group cannot interact sufficiently with the C18 stationary phase to create hydrophobic retention, leading also to very low selectivity under IP-RPLC mode. In terms of peak capacity, the values were fully comparable to what was reported in Fig. 4, with P values ranging from 14 (ZIC-cHILIC) to 27 (Amide).

3.3.3. Analysis of ONs having different number of PS linkages

Fig. 6 shows the separation of ONs with various number of PS linkages, comprised between 17 and 19. The average selectivity was again very low, with α values ranging from 1.03 (C18 column) to 1.08 (Amide and HILIC-Z), while the OH5 column offered much higher average selectivity of 1.15. With this column, an interesting separation was obtained between the species with 17 (vola-17PS) and 19 PS linkages (reference vola), but the separation of species with only one PS linkage difference remains very critical. In general, the ON with 19 PS linkages (reference vola) was better resolved from the two other species. To better understand this chromatographic behavior, it is important to keep in mind that the chemical properties of a PS molecule are different from its PO counterpart. Indeed, due to the close electronegativity of P and S atoms, PS are also less hydrophilic than PO linkages and therefore exhibit more complex secondary structure [31]. Because of these changes in the secondary structure, it is probable that the PS linkages are hidden in the structure of the ON, so the chemical interactions between PS groups and the column itself might be quite limited, leading to negligible differences in terms of chromatographic behavior whatever the mode (IP-RPLC and HILIC).

Even though the number of diastereoisomers is reduced when moving from 19 (2^{19} diastereoisomers), to 17 PS linkages (2^{17} di-

Table 4
For each selected column, chromatographic descriptors for highly modified ONs are reported, namely % of organic mobile phase composition at the elution (C_e); selectivities between the oligonucleotide and vola (reference); and peak capacities (P, calculated using the peak width @50% for each oligonucleotide). Corresponding chromatograms are provided in Fig. 4 (vola-18/19/21/22mer), Fig. 5 (vola-3/2/1/0mC), Fig. 6 (vola-18/17PS), and Fig. 7 (vola-8/9MOE).

		C18	Amide	OH5	ZIC-cHILIC	Nucleodur HILIC	HILIC-Z	Syncronis HILIC
	t_0	0.810	0.470	0.451	0.630	0.237	0.411	0.484
vola (reference)	C_e (%)	23.2	55.9	62.1	50.5	68.2	61.2	67.7
	P	20	26	21	13	19	18	20
vola-18mer	C_e (%)	22.6	56.6	62.7	51.5	68.7	61.9	68.3
	$\alpha_{/vola}$	1.24	1.17	1.23	1.24	1.14	1.19	1.13
	P	25	34	44	22	30	36	40
vola-19mer	C_e (%)	22.7	55.9	62.3	50.6	68.3	61.3	67.9
	$\alpha_{/vola}$	1.18	1.00	1.07	1.02	1.03	1.02	1.03
	P	24	33	31	16	26	23	29
vola-22mer	C_e (%)	24.0	55.7	61.7	49.5	67.9	60.5	67.4
	$\alpha_{/vola}$	1.22	1.06	1.14	1.23	1.07	1.16	1.08
	P	18	13	10	6	10	8	9
vola-21mer	C_e (%)	23.7	55.9	61.9	50.1	68.2	60.9	67.7
	$\alpha_{/vola}$	1.13	1.02	1.06	1.10	1.01	1.06	1.02
	P	18	18	13	9	12	11	13
vola-18PS	C_e (%)	23.1	55.6	61.7	50.3	68.0	60.9	67.5
	$\alpha_{/vola}$	1.03	1.07	1.11	1.06	1.04	1.08	1.06
	P	19	22	16	13	16	16	17
vola-17PS	C_e (%)	23.2	55.5	61.5	50.2	68.0	60.8	67.4
	$\alpha_{/vola}$	1.02	1.10	1.18	1.07	1.05	1.09	1.07
	P	19	24	17	13	16	16	17
vola-9MOE	C_e (%)	22.6	55.6	61.9	50.1	68.2	60.9	67.6
	$\alpha_{/vola}$	1.20	1.08	1.05	1.10	1.01	1.07	1.02
	P	21	29	23	15	21	20	22
vola-8MOE	C_e (%)	22.2	55.2	61.7	49.8	67.9	60.6	67.4
	$\alpha_{/vola}$	1.40	1.17	1.12	1.16	1.06	1.14	1.07
	P	27	36	35	18	32	30	38
vola-3mC	C_e (%)	23.1	56.0	62.2	50.4	68.4	61.2	67.9
	$\alpha_{/vola}$	1.03	1.00	1.04	1.04	1.06	1.01	1.04
	P	20	27	22	14	20	19	21
vola-2mC	C_e (%)	23.1	55.9	62.2	50.3	68.5	61.2	67.9
	$\alpha_{/vola}$	1.05	1.01	1.04	1.06	1.06	1.00	1.04
	P	19	26	22	14	20	18	21
vola-1mC	C_e (%)	23.0	55.9	62.3	50.2	68.5	61.2	67.9
	$\alpha_{/vola}$	1.07	1.02	1.05	1.07	1.07	1.00	1.05
	P	19	27	22	14	20	19	21
vola-0mC	C_e (%)	22.9	55.8	62.3	50.2	68.5	61.2	67.9
	$\alpha_{/vola}$	1.09	1.03	1.06	1.07	1.07	1.01	1.05
	P	19	29	28	16	25	25	26

astereoisomers), the difference in terms of number of diastereoisomers was too limited to significantly impact peak capacity, which still varies from 13 (ZIC-cHILIC) to 24 (amide). However, it has been recently demonstrated that suppression of diastereoisomeric separation can be obtained in IP-RPLC mode when using ion-pairing amines with moderate hydrophobicity (*i.e.* DPAA, DBAA or HAA), leading to the separation of ONs with different number of PS linkages [29]. Most probably, a different HILIC mobile phase composition could also lead to better separation of ONs with different degree of PS linkages.

3.3.4. Analysis of ONs having different number of MOE modifications

Finally, Fig. 7 shows the separation of ONs having a different number of 2′-*O*-methoxyethyl (MOE) sugar moieties modifications comprised between 8 and 10.

As reported in Table 4, the retention, expressed as C_e, was slightly higher when increasing the number of MOE modifications in IP-RPLC (higher C_e was required for the species containing the largest number of MOE modifications), meaning that the overall hydrophobicity of the product was slightly increasing with the number of MOE. In HILIC, the behavior was opposite, with a higher C_e for the species containing the largest number of MOE modifications, meaning that those species were less retained. This is logical, as more hydrophobic substances should be less retained under HILIC conditions.

The replacement of the hydrophilic 2′-hydroxyl group by 2′-*O*-methoxyethyl group increases the product hydrophobicity. Since hydrophobicity increased with the number of MOE, these species were well separated from the reference sample (vola) under IP-RPLC conditions, providing an α value of 1.20 for vola-9MOE and 1.40 for vola-8MOE. On the other hand, the average selectivity was lower in HILIC, and comprised between 1.04 (Nucleodur HILIC) and 1.13 (ZIC-cHILIC and Amide).

Interestingly, the peak capacity decreased with an increasing number of MOE modifications. Indeed, the average P values for all the seven conditions were equal to 31, 22 and 20 for vola-8MOE, vola-9MOE, and reference vola (containing 10 MOE modifications), respectively. This confirms that peak broadening was not only due to the presence of diastereoisomers related to the presence of PS linkages, but also to the presence of a significant number of MOE modifications.

4. Conclusions

Given the increasing interest for HILIC as complementary chromatographic approach to IP-RPLC for the characterization of oligonucleotides and their related impurities, the potential of zwitterionic HILIC was evaluated. For the first time, a systematic comparison between seven zwitterionic stationary phases (six sulfobetaine, one phosphorylcholine) and reference materials (*i.e.* amide, OH5 and C18) was conducted and applied to oligonucleotide analysis to prove complementarity of these stationary phases.

The columns characterization, performed through the Tanaka test by using a set of small molecules, highlighted the key retention and selectivity features that were specific for each HILIC stationary phase. In addition, it allowed to underline key differences for zwitterionic stationary phases sharing the same functional groups (sulfobetaine). Columns could be classified by their ability to retain oligonucleotides, that was estimated based on polar and anion-exchange characters. Indeed, under the reported test conditions, hydrophilic partitioning was not considered as an essential contributor to retention. As reported by McCalley et al., the water-rich layer involved in the hydrophilic partitioning is only present when the amount of water in the mobile phase is on the maximum equal to 35% [32]. In the current study, the amount of water for eluting ONs was generally comprised between 30% and 70%, depending on samples and columns. Under such conditions, the formation of the water layer to observe hydrophilic partitioning is hampered and therefore retention is mostly evaluated as driven by surface adsorption and electrostatic interactions.

Based on the Tanaka test, Z-HILIC, ZIC-cHILIC, ZIC-pHILIC and Amide were predicted to be the most retentive columns, followed by OH5 and HILIC-Z, then Syncronis HILIC, Nucleodur HILIC and Nucleoshell HILIC columns. Overall, similar selectivity profiles were obtained for Syncronis HILIC, Nucleodur HILIC and Nucleoshell HILIC, as well as for ZIC-cHILIC and ZIC-pHILIC.

Then, the HILIC stationary phases were screened for oligonucleotide analysis and results mostly confirmed the prior predictions. Z-HILIC column was even found to be too retentive for the analysis of highly polar, negatively charged compounds. Peak capacities and selectivities were discussed to evaluate overall resolution and were compared to the chromatographic performance of the C18 column operated in IP-RPLC mode. Despite very good selectivities, ZIC-cHILIC and ZIC-pHILIC provided low peak capacities that compromise their use for oligonucleotide separations. However, it is noteworthy that the other HILIC columns offered good selectivities and even better resolutions than the C18 column for unmodified oligonucleotides separations.

Therefore, when analyzing unmodified ONs, zwitterionic columns were particularly promising, with some of them (Nucleoshell HILIC and Syncronis HILIC) providing higher peak capacities than the Amide and OH5 columns, especially in the case of large ONs ($>$ 40-mer) analysis.

Finally, separations between a highly chemically modified 20-mer ON and its closely related impurities were carried out on the different stationary phases. In this case, kinetic performances and selectivities were notably decreased as compared to unmodified ONs separations, due to the highly modified sequences that only differ from one another by one or several minor modifications, and the partial diastereoisomeric separation of highly PS-modified oligonucleotides. The complementary of HILIC and IP-RPLC conditions was again demonstrated despite the smaller differences between columns. Good selectivities between ONs varying by one or two nucleotides were achieved on the ZIC-cHILIC column, while IP-RPLC remains the reference approach for length-based separations of oligonucleotides. The opposite trend was observed for the separation of phosphodiester impurities in phosphorothioate ONs. HILIC separations showed a slight improvement in selectivity as compared to IP-RPLC separation. Nevertheless, the addition of methyl groups on cytosine residues proved to have a limited impact on retention and therefore their separation resulted in limited selectivities. Considering methoxyethyl-modified oligonucleotides, IP-RPLC gave the best selectivity for these variants.

Therefore, when analyzing highly chemically-modified ONs, zwitterionic columns were not able to provide better selectivities as compared to the reference approaches (IP-RPLC or amide-/polyhydroxy fructan-bonded HILIC phases).

This contribution opens the possibility to expand the existing portfolio of chromatographic techniques to characterize oligonucleotides. By understanding column characteristics, zwitterionic HILIC columns have proved to be complementary to other HILIC materials when analyzing unmodified oligonucleotides, supporting the IP-RPLC analysis of oligonucleotides.

Declaration of Competing Interest

The authors declare that they have no known competing financial interests or personal relationships that could have appeared to influence the work reported in this paper.

CRediT authorship contribution statement

Honorine Lardeux: Conceptualization, Investigation, Data curation, Writing – original draft, Visualization. **Davy Guillarme:** Conceptualization, Resources, Writing – original draft, Writing – review & editing, Supervision, Project administration, Funding acquisition. **Valentina D'Atri:** Conceptualization, Writing – original draft, Writing – review & editing, Supervision, Project administration.

Data availability

Data will be made available on request.

Acknowledgments

The authors wish to thank Jean-Luc Veuthey from the University of Geneva for his fruitful comments and discussions, Eric Nebel and Cédric Crosnier (Agilent Technologies, France) for providing the OH5 and HILIC-Z columns used in this work, and Matthew Lauber (Waters Corporation, Milford, MA, USA) for the gift of the Amide and Z-HILIC columns used in this work.

Supplementary materials

Supplementary material associated with this article can be found, in the online version, at doi:10.1016/j.chroma.2023.463785.

Reference

[1] N. Dammes, D. Peer, Paving the road for RNA therapeutics, Trends Pharmacol. Sci. 41 (2020) 755–775, doi:10.1016/j.tips.2020.08.004.
[2] L.W. Harries, RNA biology provides new therapeutic targets for human disease, Front. Genet. 10 (2019), doi:10.3389/fgene.2019.00205.
[3] A. Rinaldi, RNA to the rescue, EMBO Rep. 21 (2020), doi:10.15252/embr.202051013.
[4] T.C. Roberts, R. Langer, M.J.A. Wood, Advances in oligonucleotide drug delivery, Nat. Rev. Drug Discov. 19 (2020) 673–694, doi:10.1038/s41573-020-0075-7.
[5] C.I.E. Smith, R. Zain, Therapeutic oligonucleotides: state of the art, Annu. Rev. Pharmacol. Toxicol. 59 (2019) 605–630, doi:10.1146/annurev-pharmtox-010818-021050.
[6] D.R. Corey, M.J. Damha, M. Manoharan, Challenges and opportunities for nucleic acid therapeutics, Nucleic Acid Ther. 32 (2022) 8–13, doi:10.1089/nat.2021.0085.
[7] M.M. Lemaitre, Individualized antisense oligonucleotide therapies: how to approach the challenge of manufacturing these oligos from a chemistry, manufacturing, and control-regulatory standpoint, Nucleic Acid Ther. 32 (2022) 101–110, doi:10.1089/nat.2021.0030.
[8] D. Capaldi, A. Teasdale, S. Henry, N. Akhtar, C. den Besten, S. Gao-Sheridan, M. Kretschmer, N. Sharpe, B. Andrews, B. Burm, J. Foy, Impurities in oligonucleotide drug substances and drug products, Nucleic Acid Ther. 27 (2017) 309–322, doi:10.1089/nat.2017.0691.
[9] D. Capaldi, N. Akhtar, T. Atherton, D. Benstead, A. Charaf, T. De Vijlder, C. Heatherington, J. Hoernschemeyer, H. Jiang, U. Rieder, F. Ring, R. Peter, J.A. Stolee, R. Wechselberger, Strategies for identity testing of therapeutic oligonucleotide drug substances and drug products, Nucleic Acid Ther. 30 (2020) 249–264, doi:10.1089/nat.2020.0878.
[10] C.J. Vanhinsbergh, Analytical separation methods for therapeutic oligonucleotides, LC/GC Eur. 33 (2020) 20–26. https://www.chromatographyonline.com/view/analytical-separation-methods-for-therapeutic-oligonucleotides.
[11] S. Pourshahian, Therapeutic oligonucleotides, impurities, degradants, and their characterization by mass spectrometry, Mass Spectrom. Rev. (2019) mas.21615, doi:10.1002/mas.21615.
[12] J.M. Sutton, G.J. Guimaraes, V. Annavarapu, W.D. van Dongen, M.G. Bartlett, Current state of oligonucleotide characterization using liquid chromatography–mass spectrometry: insight into critical issues, J. Am. Soc. Mass Spectrom. 31 (2020) 1775–1782, doi:10.1021/jasms.0c00179.

[13] A. Kilanowska, B. Buszewski, S. Studzińska, Application of hydrophilic interaction liquid chromatography coupled with tandem mass spectrometry for the retention and sensitivity studies of antisense oligonucleotides, J. Chromatogr. A 1622 (2020) 461100, doi:10.1016/j.chroma.2020.461100.

[14] A. Demelenne, M.-J.J. Gou, G. Nys, C. Parulski, J. Crommen, A.-C.C. Servais, M. Fillet, Evaluation of hydrophilic interaction liquid chromatography, capillary zone electrophoresis and drift tube ion-mobility quadrupole time of flight mass spectrometry for the characterization of phosphodiester and phosphorothioate oligonucleotides, J. Chromatogr. A 1614 (2020) 460716, doi:10.1016/j.chroma.2019.460716.

[15] P.A. Lobue, M. Jora, B. Addepalli, P.A. Limbach, Oligonucleotide analysis by hydrophilic interaction liquid chromatography-mass spectrometry in the absence of ion-pair reagents, J. Chromatogr. A 1595 (2019) 39–48, doi:10.1016/j.chroma.2019.02.016.

[16] H. Lardeux, A. Goyon, K. Zhang, J.M. Nguyen, M.A. Lauber, D. Guillarme, V. D'Atri, The impact of low adsorption surfaces for the analysis of DNA and RNA oligonucleotides – Part 2: Focus on hydrophilic interaction chromatography (HILIC), Anal. Chim. Acta. (2022).

[17] L. Gong, J.S.O. McCullagh, Analysis of oligonucleotides by hydrophilic interaction liquid chromatography coupled to negative ion electrospray ionization mass spectrometry, J. Chromatogr. A 1218 (2011) 5480–5486, doi:10.1016/j.chroma.2011.06.044.

[18] M. Huang, X. Xu, H. Qiu, N. Li, Analytical characterization of DNA and RNA oligonucleotides by hydrophilic interaction liquid chromatography-tandem mass spectrometry, J. Chromatogr. A 1648 (2021) 462184, doi:10.1016/j.chroma.2021.462184.

[19] T.H. Walter, B.A. Alden, K. Berthelette, J.A. Field, N.L. Lawrence, J. McLaughlin, A.V. Patel, Characterization of a highly stable zwitterionic hydrophilic interaction chromatography stationary phase based on hybrid organic–inorganic particles, J. Sep. Sci. 45 (2022) 1389–1399, doi:10.1002/jssc.202100859.

[20] Y. Kawachi, T. Ikegami, H. Takubo, Y. Ikegami, M. Miyamoto, N. Tanaka, Chromatographic characterization of hydrophilic interaction liquid chromatography stationary phases: Hydrophilicity, charge effects, structural selectivity, and separation efficiency, J. Chromatogr. A 1218 (2011) 5903–5919, doi:10.1016/j.chroma.2011.06.048.

[21] T. Ikegami, A. Taniguchi, T. Okada, K. Horie, S. Arase, Y. Ikegami, Functionalization using polymer or silane? A practical test method to characterize hydrophilic interaction chromatography phases in terms of their functionalization method, J. Chromatogr. A 1638 (2021) 461850, doi:10.1016/j.chroma.2020.461850.

[22] D.S. Bell, Retention and selectivity of stationary phases used in HILIC, LCGC Asia Pac. 18 (2015) 26–32 https://www.chromatographyonline.com/view/retention-and-selectivity-stationary-phases-used-hilic-1.

[23] M. Gilar, K.D. Berthelette, T.H. Walter, Contribution of ionic interactions to stationary phase selectivity in hydrophilic interaction chromatography, J. Sep. Sci. 45 (2022) 3264–3275, doi:10.1002/jssc.202200165.

[24] D.V. McCalley, Is hydrophilic interaction chromatography with silica columns a viable alternative to reversed-phase liquid chromatography for the analysis of ionisable compounds? J. Chromatogr. A 1171 (2007) 46–55, doi:10.1016/j.chroma.2007.09.047.

[25] U.D. Neue, K. Tran, A. Méndez, P.W. Carr, The combined effect of silanols and the reversed-phase ligand on the retention of positively charged analytes, J. Chromatogr. A 1063 (2005) 35–45, doi:10.1016/j.chroma.2004.11.096.

[26] J. Bagge, M. Enmark, M. Leśko, F. Limé, T. Fornstedt, J. Samuelsson, Impact of stationary-phase pore size on chromatographic performance using oligonucleotide separation as a model, J. Chromatogr. A 1634 (2020) 461653, doi:10.1016/j.chroma.2020.461653.

[27] M. Gilar, K.J. Fountain, Y. Budman, U.D. Neue, K.R. Yardley, P.D. Rainville, R.J. Russell II, J.C. Gebler, Ion-pair reversed-phase high-performance liquid chromatography analysis of oligonucleotides, J. Chromatogr. A 958 (2002) 167–182, doi:10.1016/S0021-9673(02)00306-0.

[28] T. Chen, S. Tang, Y. Fu, J.G. Napolitano, K. Zhang, Analytical techniques for characterizing diastereomers of phosphorothioated oligonucleotides, J. Chromatogr. A 1678 (2022) 463349, doi:10.1016/j.chroma.2022.463349.

[29] Z. Kadlecová, K. Kalíková, E. Tesařová, M. Gilar, Phosphorothioate oligonucleotides separation in ion-pairing reversed-phase liquid chromatography: Effect of ion-pairing system, J. Chromatogr. A 1676 (2022) 463201, doi:10.1016/j.chroma.2022.463201.

[30] M. Enmark, M. Rova, J. Samuelsson, E. Örnskov, F. Schweikart, T. Fornstedt, Investigation of factors influencing the separation of diastereomers of phosphorothioated oligonucleotides, Anal. Bioanal. Chem. 411 (2019) 3383–3394, doi:10.1007/s00216-019-01813-2.

[31] M. Gilar, A. Belenky, D.L. Smisek, A. Bourque, A.S. Cohen, Kinetics of phosphorothioate oligonucleotide metabolism in biological fluids, Nucleic Acids Res. 25 (1997) 3615–3620, doi:10.1093/nar/25.18.3615.

[32] D.V. McCalley, U.D. Neue, Estimation of the extent of the water-rich layer associated with the silica surface in hydrophilic interaction chromatography, J. Chromatogr. A 1192 (2008) 225–229, doi:10.1016/j.chroma.2008.03.049.